

1 Spatial interpolation techniques for a near 2 real-time mapping of Pressure and 3 Temperature data

4 Ilaria Ferrando¹, Pierluigi De Rosa², Bianca Federici¹, and Domenico
5 Sguerso¹

6 ¹Laboratory of Geomatics, Geodesy and GIS, Department of Civil, Chemical and
7 Environmental Engineering, University of Genoa, Italy

8 ²Department of Physics and Geology, University of Perugia, Italy - Via Faina, 4 –
9 Perugia, Italy 06100

10 ABSTRACT

11 Among the different techniques for atmosphere monitoring, the GNSS (Global Navigation Satellite
12 System) can provide an innovative contribution (Bevis et al., 1992; Crespi et al., 2004; Sguerso et al.,
13 2013, 2015). The Laboratory of Geomatics, Geodesy and GIS of the University of Genoa has identified a
14 GIS procedure and a simplified physical model to monitor the Precipitable Water Vapour (PWV) content,
15 using data measured by existing infrastructures. The starting points are local estimations of Zenith Total
16 Delay (ZTD) from a GNSS Permanent Stations (PSs) network, a Digital Terrain Model (DTM) and local
17 Pressure (P) and Temperature (T) measurements (Sguerso et al., 2014; Ferrando et al., 2016). The
18 present paper shows the study of the most appropriate interpolation technique for P and T data to create
19 PWV maps in a quick, stable and automatic way, to support the monitoring of intense meteorological
20 events for both a posteriori and near real-time applications. The resulting P and T maps were compared
21 to meteorological re-analysis, to check the reliability of the simplified physical model. Additionally, the
22 Regression Kriging (RK) was employed to evaluate the data correlation with elevation and to study the
23 applicability of the technique.

24 Keywords: Environmental data interpolation, Meteorological re-analysis, Regression kriging

25 INTRODUCTION

26 To understand the role of Precipitable Water Vapour (PWV) in monitoring severe meteorological events,
27 2D distribution of P and T has to be produced starting from local observations: this is made possible by
28 means of data interpolation and a simplified physical model, owned by the Laboratory of Geomatics,
29 Geodesy and GIS (Sguerso et al., 2014; Ferrando et al., 2016), already applied in few test cases.

30 The choice of the most appropriate interpolation technique, according to the spatial distribution of
31 data, is surely a key issue. Different interpolation techniques were employed, in order to find the most
32 suitable for automatic and fast interpolation. Additionally, the interpolated P and T maps were compared
33 with P and T fields coming from re-analysis, produced by meteorological model analysing past events
34 using the whole set of measured meteorological data. The case study is the severe meteorological event
35 occurred on 4th November 2011 in Genoa (Italy).

36 The adequacy of the interpolation technique to reproduce P and T fields is treated in the first two
37 sections. The final section is dedicated to the geostatistical interpolation of data by means of Regression
38 Kriging (RK).

39 DATA AND DETERMINISTIC INTERPOLATION TECHNIQUES

40 53 Pressure and 58 Temperature NOAA meteorological stations (www.noaa.gov) were used for the
41 interpolation. Figure 1 shows the spatial distribution of P (circles) and T (crosses) stations, covering
42 approximately north-west of Italy and the French-Italian border region, with a mean spacing of 150

43 km. 4 stations, called "checkpoints" and displayed in figure 1 as small triangles, were excluded in the
44 interpolation and used to verify the accordance between interpolated and re-analysed fields.

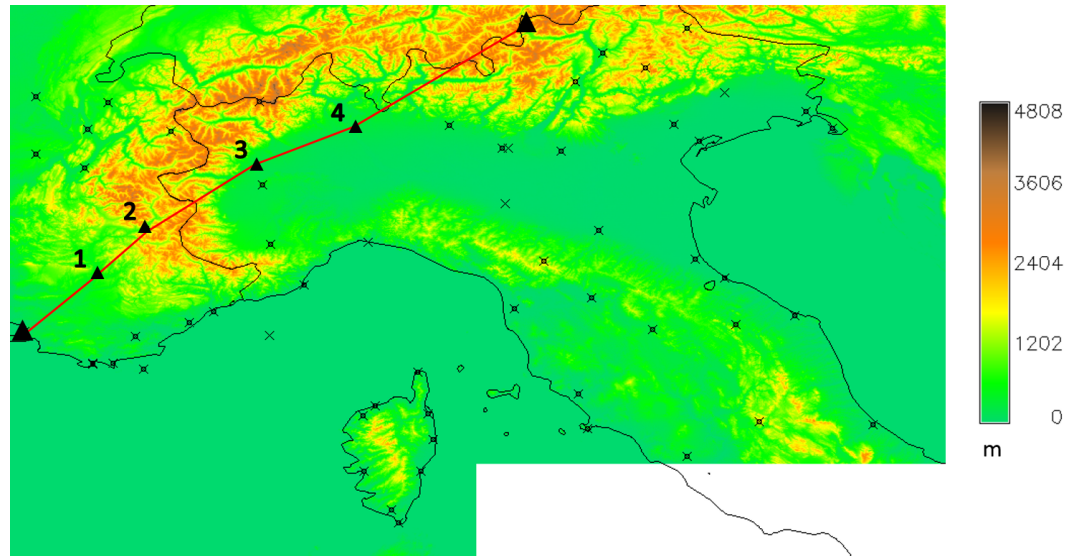


Figure 1. Distribution of P (circles) and T (crosses) stations. The transect crossing the checkpoints (small triangles) is displayed in red.

45 The interpolation was carried out at a resolution of about 3.5 km, accordingly to the one used for
46 re-analysis. The 2D maps obtained by Inverse Distance Weighted (IDW), Regularized Spline with Tension
47 (RST) and Triangulated Irregular Network (TIN) techniques for P and T are shown in figure 2, on top and
48 bottom respectively.

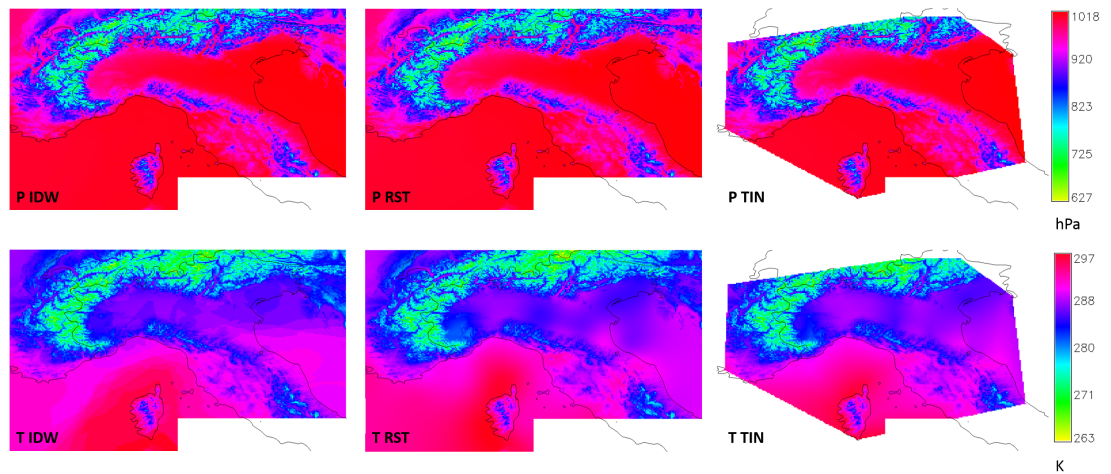


Figure 2. P (top) and T (bottom) fields obtained using IDW, RST and TIN interpolation techniques.

49 COMPARISON WITH RE-ANALYSIS

50 Two different comparisons were carried out for the interpolated maps obtained in the previous section:
51 along the transect to locally check the adherence with the re-analysis and measured data, and 2D
52 differences maps between the re-analysis and the interpolated fields to evaluate the global behaviour in
53 the study area.

54 **1D comparison: behaviour along the transept**

55 The transept passes across 4 meteorological station (the checkpoints). Figure 3 shows the values along the
56 transept of P and T respectively, for IDW, RST, TIN, re-analysis and NOAA observed data.

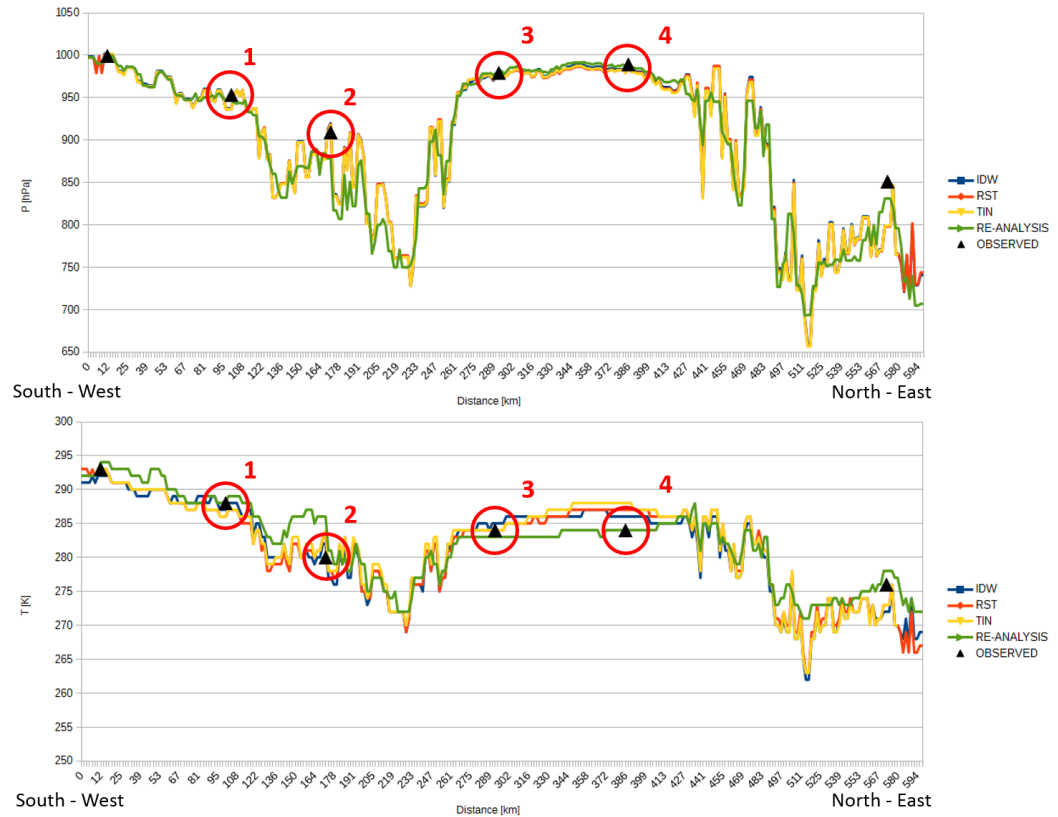


Figure 3. P (top) and T (bottom) values along the transept.

57 The interpolated maps seem quite similar along the transept. The accordance between re-analysis,
58 observed data and interpolated fields is good, in the checkpoints too, showing that it is possible to obtain
59 P and T fields even from sparse data. The major differences occur in high altitude areas, probably due to
60 the generalization of the adopted model. P seems to be more complying to re-analysis and observed data
61 than T. Focusing on the checkpoints, the maximum difference between re-analysis and interpolated fields
62 are around 40 hPa in checkpoint 2 for all the applied techniques, and 4 K for checkpoint 4 for TIN. It
63 should be noted that on checkpoint 2 there is a disagreement between re-analysis and P observed data,
64 this is maybe the cause of the previously mentioned high differences. Finally, high differences can be
65 noticed on the edge regions, due to the different behaviours of the interpolation techniques.

66 **2D comparison: difference maps**

67 The higher differences are located in high altitude areas, both for P (top of figure 4) and T (bottom of
68 figure 4) and in the edge regions, confirming what previously noted along the transept.

69 Especially in T maps, differences due to the patterns of interpolators can be seen. These differences
70 are in the order of few K, thus they are not considered influential in the description of the field. Differently,
71 as shown in the top of figure 4, not negligible differences (max=66 hPa; min=-85 hPa) are present in
72 P field around Genoa. This could be caused by the generalization of the simplified model, not capable
73 to describe local strong variations and to the absence of P data in the area. As already noted (Ferrando
74 et al., 2016), the presence of these differences don't influence the interpretation of PWV and its evolution
75 in time, thus the procedure is considered reliable for severe meteorological events monitoring. Again,
76 the global behaviour of the different interpolators seems to be similar, except for the already mentioned
77 pattern, typical of each technique.

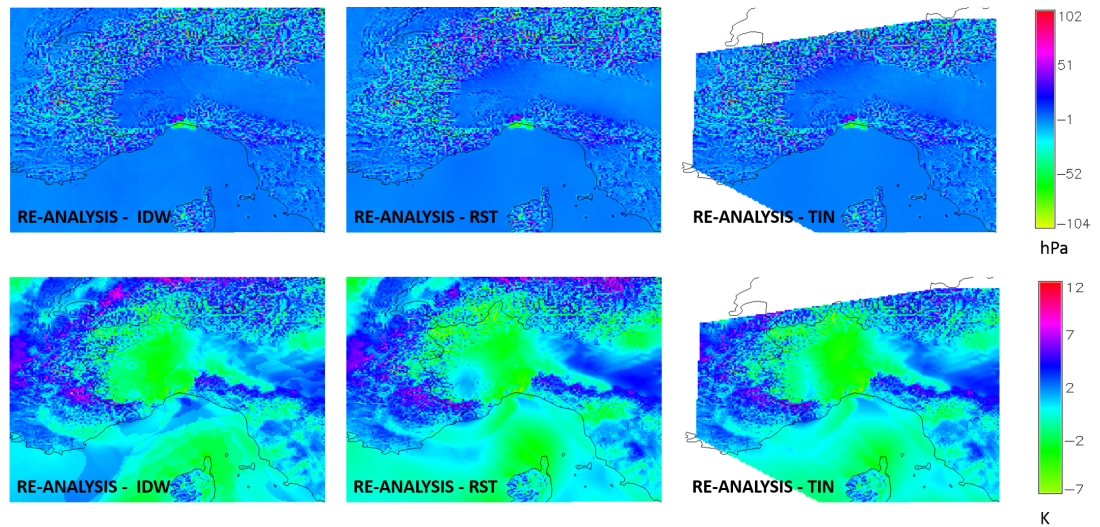


Figure 4. P (top) and T (bottom) differences.

78 Considering the application of this procedure in near real-time, the interpolator should be fast and
 79 automatically adjustable to the different network configurations that may change in time. For this reason,
 80 TIN interpolator, available as GRASS add-on by means of *r.surf.nnbathy* module (Sieczka and GRASS
 81 Development Team, 2006; GRASS Development Team, 2016), was chosen to produce PWV maps, for its
 82 adaptability and for not needing to calibrate additional parameters.

83 In the next section, a geostatistical analysis for P and T data is performed.

84 GEOSTATISTICAL INTERPOLATION

85 P and T data show a strong correlation with elevation as figure 5 shows. For such reason, the Regression
 86 Kriging (RK) (Hengl et al., 2007) could be the best interpolation technique as it is able to use elevation
 87 information as base data for interpolate Pressure and Temperature values. The ASTER GDEM digital
 88 elevation model has been used as raster layer providing the auxiliary variable in order to interpolate the
 89 regression residuals.

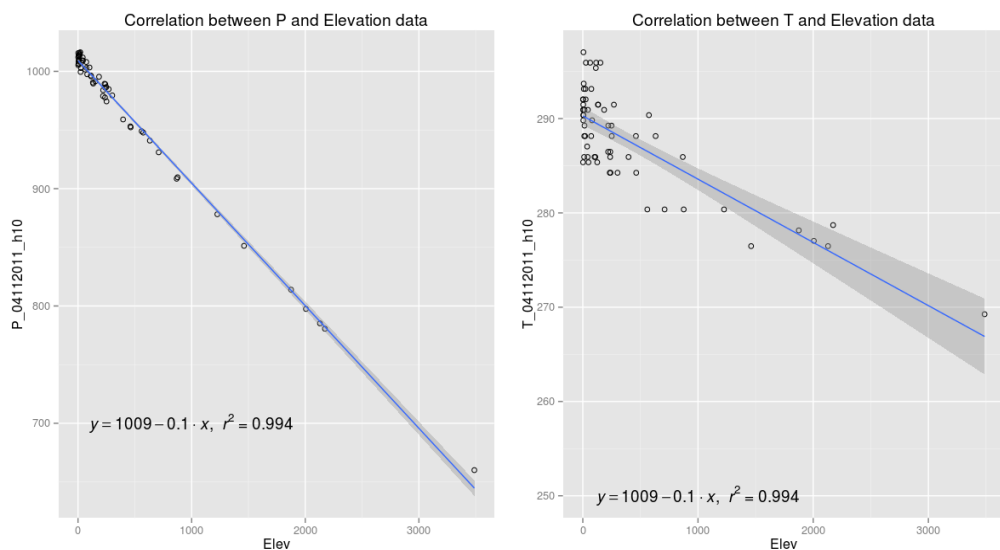


Figure 5. Correlation between P and T values versus elevation data.

90 The goodness of the RK analysis could be observed in figure 6: on the left, the bubbles of the cross
 91 validation procedure of IDW, using 5 k-folds; on the right, the bubble plot of RK interpolation. It turns
 92 out how the IDW has a range of errors much wider than RK, also the location of residuals error is not
 93 similar in both cases: IDW shows biggest errors in Alpine and in Apennines regions, whereas RK shows
 94 the biggest residual errors only in Alpine region.

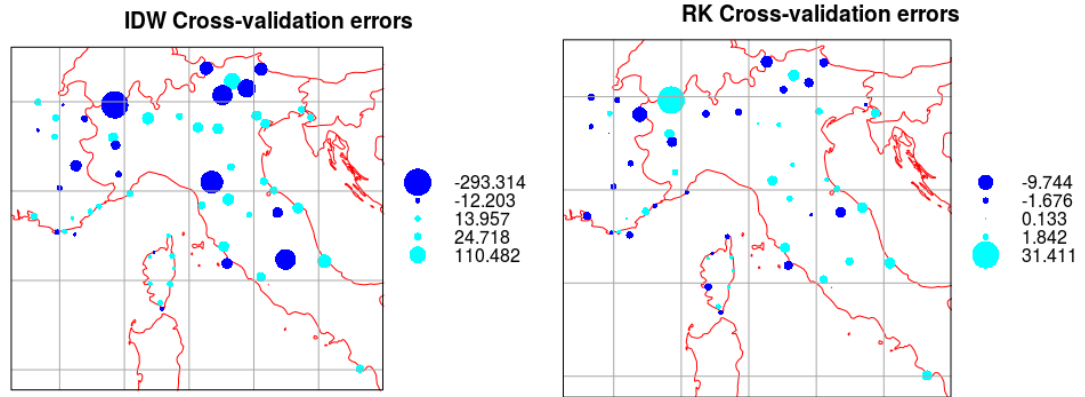


Figure 6. Bubble plots comparing the IDW (left) and RK interpolation methods (right) using a 5 k-folds cross validation procedure.

95 The RK interpolation has been implemented into R statistical software (R Core Team, 2016) using
 96 gstat and intamap packages (Pebesma, 2004; Pebesma et al., 2010). In particular, a R code has been
 97 produced to run the procedure automatically. The code is able to load P and T data, execute the variogram
 98 analysis of the dependent variables on auxiliary variables (elevation from ASTER GDEM) and compute
 99 the interpolated raster for P and T and relative map of kriging errors.

100 CONCLUSIONS AND FUTURE DEVELOPMENTS

101 A deep analysis of the different interpolation techniques was carried out, in order to find the most
 102 appropriate for near real-time applications too. Despite the difficulties due to the sparse distribution of
 103 P and T data and the considerable orographic effect, the simplified physical model implemented by the
 104 Laboratory of Geomatics, Geodesy and GIS is reliable to produce 2D PWV maps with good adherence
 105 to re-analysis. The geostatistical analysis of data helped in analysing the correlation between data and
 106 elevation, computing the interpolated maps and evaluating the errors. The comparison between P and T
 107 Kriging maps, the deterministic interpolated maps and the re-analysis will be carried out in the future
 108 complete paper.

109 ACKNOWLEDGMENTS

110 Thanks to Federico Cassola and PM_TEN srl (DIFI, Department of Physics, spin-off of University of
 111 Genoa) and to Andrea Mazzino (DICCA, Department of Civil, Chemical and Environmental Engineering,
 112 University of Genoa) for sharing the re-analysis data.

113 REFERENCES

- 114 Bevis, M., Businger, S., Herring, T. A., Rocken, C., Anthes, R. A., and Ware, R. H. (1992). Gps
 115 meteorology: Remote sensing of atmospheric water vapor using the global positioning system. *Journal*
 116 *of Geophysical Research: Atmospheres*, 97(D14):15787–15801.
 117 Crespi, M., Luzietti, L., Frattale Mascioli, F. M., and Rizzi, A. (2004). Impiego meteorologico del gps per
 118 la previsione di precipitazioni critiche. In *Atti della 8 Conferenza Nazionale ASITA*. ASITA.
 119 Ferrando, I., Federici, B., and Sguerso, D. (2016). Environmental data interpolation to support GNSS
 120 monitoring of potential precipitation. *Geomatics Workbooks*, 13. (accepted for publication, under
 121 revision).

- 122 GRASS Development Team (2016). *Geographic Resources Analysis Support System (GRASS GIS)*
123 *Software, Version 7.0*. Open Source Geospatial Foundation.
- 124 Hengl, T., Heuvelink, G. B., and Rossiter, D. G. (2007). About regression-kriging: from equations to case
125 studies. *Computers & Geosciences*, 33(10):1301–1315.
- 126 Pebesma, E., Cornford, D., Dubois, G., Heuvelink, G., Hristopoulos, D., Pilz, J., Stoeckler, U., Morin,
127 G., and Skoien, J. (2010). Intamap: the design and implementation of an interoperable automated
128 interpolation web service. *Computers & Geosciences*, 37:343–352.
- 129 Pebesma, E. J. (2004). Multivariable geostatistics in s: the gstat package. *Computers & Geosciences*,
130 30:683–691.
- 131 R Core Team (2016). *R: A Language and Environment for Statistical Computing*. R Foundation for
132 Statistical Computing, Vienna, Austria.
- 133 Sguerso, D., Federici, B., Agrillo, G., and Ferrando, I. (2014). Il contributo della geomatica alla
134 valutazione delle allerte meteorologiche. *Newton's Bulletin*, Vol. II prof. Sansò e l'evoluzione della
135 geodesia in Italia, CD-ROM:1–11.
- 136 Sguerso, D., Labbouz, L., and Walpersdorf, A. (2013). 14 years of gps tropospheric delays in the french-
137 italian border region: a data base for meteorological and climatological analyses. In *International*
138 *Workshop "The Role of Geomatics in Hydrogeological Risk"*.
- 139 Sguerso, D., Labbouz, L., and Walpersdorf, A. (2015). 14 years of gps tropospheric delays in the
140 french–italian border region: comparisons and first application in a case study. *Applied Geomatics*,
141 8(1):13–25.
- 142 Sieczka, M. and GRASS Development Team (2006). *r.surf.nnbathy GRASS Software, Version 6.4.*. Open
143 Source Geospatial Foundation.